Journal of Materials Chemistry A

Accepted Manuscript

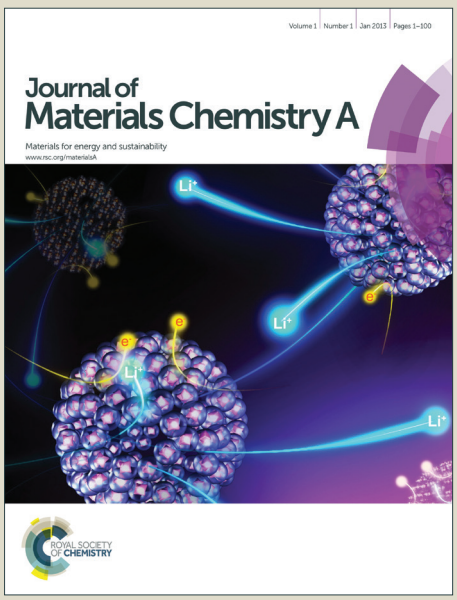

ROYAL SOCIETY OF CHEMISTRY

www.rsc.org/materialsA

Journal Name

RSCPublishing

ARTICLE

Novel POSS-based Organic-Inorganic Hybrid Porous Materials by Low Cost Strategy

Cite this: DOI: 10.1039/xoxxoooooox

Shaolei Wang,[a] Liangxiao Tan,[a] Chengxin Zhang,[a] Irshad Hussain,[c] and Bien Tan*[a,b]

Received ooth January 2012,
Accepted ooth January 2012

DOI: 10.1039/xoxxoooooox

www.rsc.org/

Two kinds of POSS-based organic-inorganic hybrid porous materials have been synthesized *via* Friedel–Crafts and Scholl coupling reactions, for the first time, using low-cost building blocks i.e., Octaphenylsilsesquioxanes and simple knitting approaches to obtain high Burnauer-Emmett-Teller (BET) surface area porous polyhedral oligomeric silsesquioxanes (POSS)-based hybrid materials. N_2 sorption isotherms of polymers show that both of these materials are predominantly microporous and mesoporous with BET surface area of 795 $m^2 g^{-1}$ for polymer of Octaphenylsilsesquioxanes-1 (POPS-1) and 472 $m^2 g^{-1}$ for polymer of Octaphenylsilsesquioxanes-2 (POPS-2). Moreover, the POPS-1 can reversibly adsorb 9.73 wt% CO_2 (1 bar and 273 K) and 0.89 wt% H_2 (1.13 bar and 77 K), and POPS-2 shows moderate gas uptake with 8.12 wt% CO_2 (1 bar and 273K) and 0.64 wt% H_2 (1.13 bar and 77 K), respectively. In addition, the integrity structure of POSS based building blocks was completely preserved under relatively strong acidic conditions.

Introduction

The porous materials have attracted great scientific interest, due to their potential applications in gas storage[1], separation,[2] heterogeneous catalysis,[3] low-k dielectrics,[4] chemical sensing,[5] and energy storage[6] *etc*. The traditional porous materials, zeolites and activated carbon with high mechanical strength and thermal stability play important role in the above-mentioned fields, however, the difficulty in their post-functionalization usually limit their applications.[7] Apart from these traditional porous materials, microporous organic polymers (MOPs), which possess the advantages of light skeletal density, diverse synthetic routes and easier functionalization, have also attracted significant attention.[8] During the last decade, many of the novel MOPs have been reported such as polymers of intrinsic microporosity (PIMs),[9] covalent organic frameworks (COFs),[10,11] conjugated microporous polymers (CMPs),[12,13] hypercrosslinked porous polymers (HCPs),[14,15] and porous aromatic frameworks (PAFs).[16] However most of the MOPs usually lack the desired mechanical strength and high thermal stability for practical applications. The combination of organic with inorganic moieties generally results in porous hybrid materials with diverse structures and thus offers novel research perspectives to develop promising functional materials. Metal organic frameworks (MOFs) show several advantages such as high surface area and gas uptake, [17] but their poor hydrothermal stability limits their practical applications.[18]

Porous POSS-based materials, a novel class of organic-inorganic hybrid materials, show high thermal/hydrothermal stability and offer easier post-synthesis functionalization, opening a promising research area to produce practically effective materials for most of the above-mentioned applications.[19, 20]

Polyhedral oligomeric silsesquioxanes (POSS) ($R_8Si_8O_{12}$, R=H or organic groups) are a novel kind of nanoscale organic-inorganic hybrid molecules, which possess a double-four-ring (D4R) cage structure.[21] POSS and its derivatives with hyper-branched geometry, rigidity, easier functionalization and high symmetry are ideal building blocks to design and produce interesting organic-inorganic hybrid porous materials for various applications.[22]

Recently, more porous POSS-based networks have been reported with high surface areas by linking functionalized POSS units through diverse reactions.[7,19,22-30] Zhang *et al*. reported POSS-based hybrid porous materials with an S_{BET} of 380 $m^2 g^{-1}$ to 530 $m^2 g^{-1}$, which were formed by hydrosilation reaction using octavinylsilsesquioxane (OVS) and octahydrosilsesquioxane as precursors.[30] Morrison *et al*. also prepared POSS-based hybrid porous materials by hydrosilation using OVS as important building units, and further carried out their functionalization by "ring opening" under triflic acid or hydroxide.[26] However, the flexible aliphatic chains are prone to efficient packing of building blocks in the polymer structure to reduce their surface area and affect their thermal stability and mechanical strength. Microporous organic-inorganic hybrid materials with high thermal stability and surface area were also synthesized using para-iodinated octaphenylsilsesquioxane as building units by Ullmann homo-coupling or Suzuki cross-coupling reactions. [24,27] Okubo *et al*. synthesized poly(organosiloxane) networks (PSNs) materials with high surface area employing bromophenyl-ethenylterminated D4R cages as basic building blocks by higher level of crosslinking and longer rigid linker distance.[7,31] Using the benzyl chloride-terminated D4R cage as precursors *via* Friedel-Crafts self-condensation, Chaikittisilp *et al*. reported the highest surface area (up to 2500 $m^2 g^{-1}$) for siloxane-based materials.[19] Liu *et al*. employed Heck cross-coupling reactions to

prepare a series of organic-inorganic hybrid porous polymers (HPPs) using OVS as precursors.[20,29] Liu *et al* also synthesized other HPPs materials using OVS and benzene as monomers by Fridel-Craft reaction.[32] Moreover, POSS-based porous materials were also reported using octa(aminophenyl)-silsesquioxane as basic building units.[28,33] However, there are still several problems for the production of POSS-based hybrid porous materials: 1) the synthesis of ideal POSS derivatives is complicated and require multiple cumbersome steps, 2) the requirement of expensive noble metal catalysts, 3) and the partial cleavage of the D4R cage structure in hybrid materials.[19,20,22,29] Recently, some simple and relatively low-cost POSS-based hybrid porous polymers were also synthesized *via* thiol-ene "click" chemistry and hydrogenation reaction.[22,23,34] Therefore, the development of simple, reproducible and cost-effective approaches for the synthesis of porous organic-inorganic hybrid material using relatively cheaper POSS-based monomers is highly desired for their practical applications.

In 2011, our group reported a versatile and flexible method to prepare hypercrosslinked microporous polymers by employing a simple one-step Friedel-Crafts reaction using formaldehyde dimethyl acetal (FDA) as an external cross-linker.[14] Recently, a new approach has been developed to obtain microporous polymers by employing Scholl reaction to form a new aryl-aryl bond in the presence of Friedel-Crafts catalyst.[35] These reactions are very useful for "knitting" aromatic rings, and offer cost-effective, versatile and flexible methods for the synthesis of porous polymers.[2,36-38]

In this paper, we employed these two synthetic strategies to crosslink octaphenyl POSS (OPS) to obtain low-cost and high surface area microporous POSS-based polymers, which offer a low-cost and facile way for the production of high surface area organic-inorganic hybrid porous materials. The resulting porous materials, POPS-1 and POPS-2, show high surface area and thermal stability. The POSS-based organic-inorganic hybrid porous materials are thoroughly characterized to understand their structure and gas adsorption properties.

Experimental section

Octaphenylsilsesquioxane and formaldehyde dimethyl acetal (FDA) was purchased from Aladdin chemical reagent Corp (shanghai, china) and used as received. 1, 2-dichloroethane, chloroform, methanol, ethanol, anhydrous ferric chloride and anhydrous aluminium chloride were obtained from Sinopharm chemical reagent Co., Ltd (shanghai, china) and used as received. Unless otherwise noted, all reagents were obtained from commercial suppliers and used without further purification.

Synthesis of POPS-1 by knitting method with external crosslinker (FDA)

Under nitrogen atmosphere, the anhydrous ferric chloride (24 mmol, 3.89 g) was added to a solution of OPS (1mmol, 1.033g) and FDA (24 mmol, 1.83g) in 1, 2-dichloroethane (DCE, 16 ml). The resulting mixture was heated at 45 °C for 5 h and then at 80 °C for 19 h. After cooling, the solid product was washed with methanol three times, further purified by extracting with methanol for 24 h, and finally dried in a vacuum oven at 60 °C for 24 h. The polymer material was obtained as a dark brown solid. Yield: 98 % (Equation S1, ESI†).

Synthesis of POPS-2 by Scholl coupling

Under nitrogen atmosphere, OPS (1 mmol, 1.033 g) was dispersed for 20 min in $CHCl_3$ (8 ml), and then anhydrous $AlCl_3$ (16 mmol, 2.13 g) was added to the solution at 60 °C. The resulting mixture was heated at 60 °C for 24 h. After cooling, the solid product was quenched using HCl:H_2O (v/v = 2:1), washed three times with ethanol, further purified by extracting with ethanol for 24 h, and finally dried in a vacuum oven at 70 °C for 24 h. The polymer material was obtained as a yellow solid. Yield: 96 % (Equation S1, ESI†).

FT-IR and Solid NMR experiments

FT-IR spectra were recorded by using a Bruker VERTEX 70 FT-IR Spectrometer employing KBr disk method. Solid-state ^{13}C CP/MAS NMR and ^{29}Si MAS NMR spectra were obtained on a WB 400 MHz Bruker Avance II spectrometer. The ^{13}C CP/MAS NMR spectra were collected with a spinning rate of 8 kHz, and using a 4mm double-resonance MAS probe. The ^{29}Si CP/MAS NMR spectra were collected with a spinning rate of 5 kHz, and using a 7 mm double-resonance MAS probe.

TGA, SEM and HRTEM analysis

Thermogravimetric analysis (TGA) was performed from room temperature to 850 °C under nitrogen, employing a PerkinElmer Instrument Pyris1 TGA with a heating rate of 10 °C/min. The field-emission scanning electron microscopy (FE-SEM) images were recorded employing a FEI Sirion 200 field-emission scanning electron microscope operated at 10 kV. Before measurement, the samples were dried in a vacuum oven at 70 °C for 24 h and then sputter coated with platinum. The high resolution transmission electron microscopy (HRTEM) images were recorded on a Tecnai G2 F30 microscope (FEI Corp. Holland) operated at 200 kV.

Gas adsorption measurements

Gas (H_2, N_2, CO_2) sorption properties and specific surface area of samples were measured using a Micromeritics ASAP 2020 surface area and porosity analyzer. Before analysis, the samples were degassed at 110 °C for 8 h under vacuum of 10^{-5} bar. Pore size distribution was calculated by N_2 adsorption isotherm employing tarazona nonlocal density functional theory (NLDFT) model assuming slit pore geometry. Total pore volumes (V_{toal}) were derived from nitrogen sorption isotherms at relative pressure P/P_0=0.995.

Results and discussion

Following the POSS-based porous materials reported, [30] these novel materials attracted much attention to improve their synthesis and explore new applications. High-cost synthesis and the partial cleavage of D4R are the two serious problems during the POSS-based porous networks preparation process.[7, 19, 22]

Due to the chemical nature of rigid POSS units and harsh reactive conditions, structural stress is usually introduced during the synthesis of POSS-based porous materials affecting the integrity of D4R structure. Soft linking units and low degree of hyper-crosslinking may release the structural stress to keep the integrity of D4R structure. So, we tried to introduce soft methylene linker into the rigid and highly symmetrical OPS building blocks to release the structural stress and keep the integrity of D4R structure through simple Fridel-Craft reaction with external crosslinker; and the steric effect during the Scholl

coupling reaction also reduced the degree of hyper-crosslinking to yield the same result.

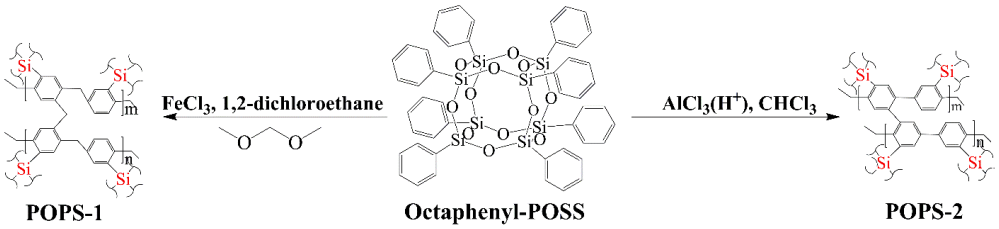

Scheme 1. The synthetic pathway to the network structure

As shown in scheme 1, the two novel organic-inorganic hybrid porous materials were prepared by using low-cost OPS through simple Friedel-Crafts reaction with external crosslinker and Scholl coupling reaction. In order to confirm the integrity of POSS D4R cage structure, FITR and ^{29}Si MAS NMR are the most reliable characterization tools.[7,19,20,31,34] Compared to the FITR spectra of the monomer OPS, the peak for the strong Si-O-Si stretching vibrations is also observed at 1100 cm^{-1} in POPS-2, confirming the presence of D4R cage (Fig. S2 and S3, ESI†).[21] However, the Si-O-Si stretching vibrations of POPS-1 shifts to the lower wave number, and Si-OH vibration appears at 950 cm^{-1}, which suggest the partial cleavage of the D4R cage in hybrid materials.[22, 26]

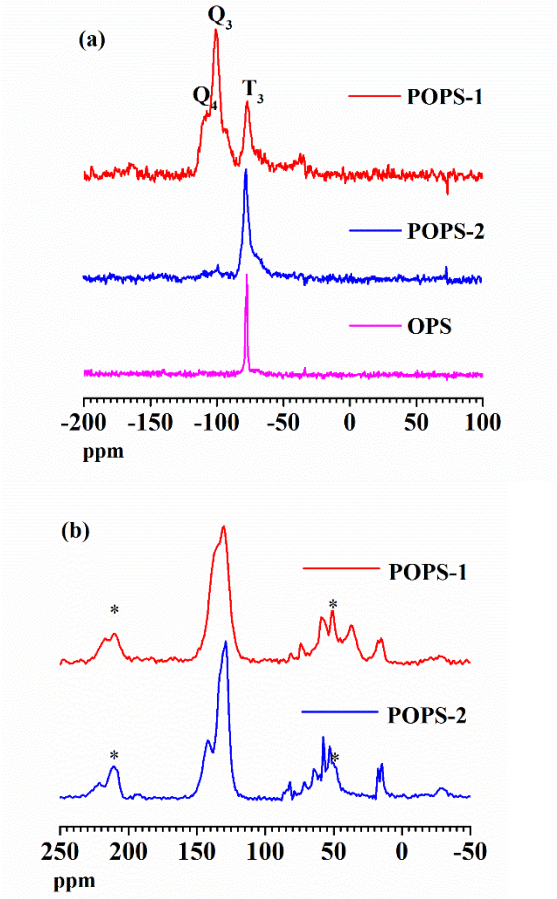

Figure 1. The solid ^{29}Si (a) and ^{13}C (b) MAS NMR spectra of OPS, POPS-1 and POPS-2

The solid-state ^{29}Si MAS NMR spectroscopy was employed to further confirm the integrity of POSS D4R cage structure of these two networks (Fig. 1a). Based on the reported ^{29}Si NMR spectroscopy of POSS-based porous network, due to the collapse of D4R cage, the polymer should possess three signals, which are attributed to the T_1, T_2 and T_3 units (T_n: $CSi(OSi)_n(OH)_{3-n}$).[7,19,31] The T_3 peak represent the Si resonance in the intact D4R cage, while the appearance of T_1 or T_3 peaks means the collapse of partial D4R cages. The spectra of OPS showed a T_3 peak at -77 ppm, which are consistent with the reported chemical shifts.[21]. The spectra of POPS-1 with T_3 peak at -77 ppm, also show a Q_3 peak at -100 ppm and a Q_4 peak at -110 ppm which should be ascribed the Q type peak (Q_n: $Si(OSi)_n(OH)_{4-n}$) in the range -90 to -120 ppm and indicates the breakage of C-Si bond.[19,20,22,24,27,34,39-42] Unlike POPS-1, the structural integrity of D4R cage is maintained in POPS-2, whose spectra show only one peak of T_3.[20,29] Based on the above FTIR and ^{29}Si NMR data, to our surprise, the D4R cage structure of POSS showed better structural integrity in POPS-2 than that of POPS-1 under harsh conditions. It may be due to the structural stress from high degree of hyper-crosslinking in POPS-1 that may force D4R cage cleavage and breakage of C-Si bond, [19,41] while in the Scholl coupling reaction, the steric effect decreases the degree of hyper-crosslinking in POPS-2, thus easing the structural stress leading to less structure cleavage.

Compared with to the FTIR spectra of OPS, POPS-1 and POPS-2, we can find observe that the C-H stretching vibrations of aromatic ring at 3100-3000 cm^{-1} disappeared after reactions (Fig. S2 and S3, ESI†) in both POPS-1 and POPS-2. It means the aromatic ring of OPS takes part in reactions. the ^{13}C CP/MAS NMR chemical shifts of POPS-1 and POPS-2 were observed at δ=130 ppm, 137 ppm and 36 ppm, which were attributed to unsubstituted aromatic carbon, substituted aromatic carbon and carbon in the methylene linker formed after Friedel-Crafts reaction or Scholl coupling reaction, respectively (Fig. 1b).[14,35] From FTIR and ^{13}C CP/MAS NMR of porous materials, we can confirm that the OPS was effectively crosslinked to form porous polymer materials via Friedel–Crafts and Scholl coupling reactions, respectively.

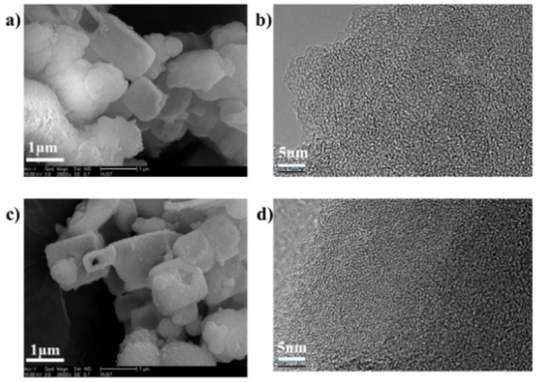

Figure 2. The FE-SEM image (a) and HRTEM image (b) of POPS-1; the FE-SEM image (c) and HRTEM image (d) of POPS-2.

The thermal stabilities of OPS and its polymers were recorded by thermogravimetric analysis (TGA) (Fig. S4, ESI†). The OPS showed obvious loss near 450 °C, which was ascribed to the loss of phenyl group.[34] Due to the partial cleavage of D4R structure, compared to the other MOPs, POPS-1 and POPS-2 exhibited moderate thermal stability without thermal degradation only up to 350 °C.[1,13,15,16,36] In addition, due to the introduction of methylene linker into the materials structure, the residue of POPS-1 is higher than those of POPS-2 and OPS. The morphologies and textures of the two networks were investigated by FE-SEM and HRTEM (Fig. 2 and Fig. S1, ESI†). The OPS showed similar hexahedral structure, while the polymers were found to possess irregular blocks-like shapes, with particle size of over 100 nm, with abundant microporous and mesoporous structure.[19, 34] (Fig. 2b and 2d)

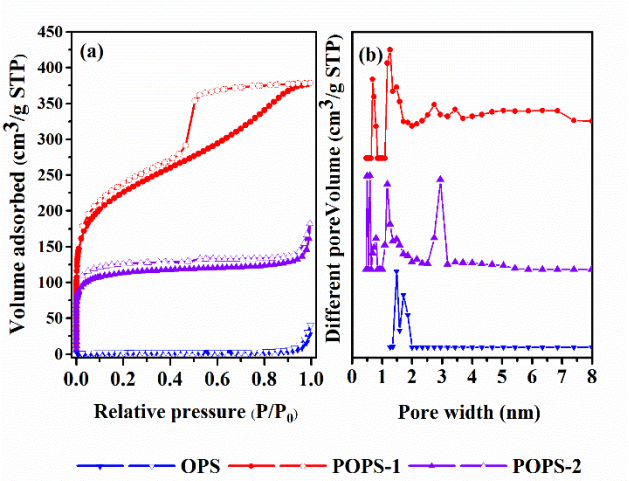

Figure 3. Nitrogen adsorption and desorption isotherm at 77.3 K (a) and pore distribution of pore size distribution calculated using DFT methods (slit pore models, differential pore volumes). Pore width (b) of samples.

After confirming abundant porous structure of polymers by HRTEM, the porous nature of polymers was further investigated by N_2 sorption analysis at 77 K (Fig. 3). Figure 3a shows that the nitrogen sorption isotherm of OPS shows a type Ⅱ character.[43, 44] Unlike the sorption isotherms of the OPS, the adsorption isotherms of POPS-1 and POPS-2 exhibited a type Ⅰ character with a high nitrogen gas uptake at low relative pressure ($P/P_0 < 0.001$), thus indicating abundant microporous structure, which is consistent with the result of HRTEM. Compared to POPS-2, the isotherm of POPS-1 showed very obvious hysteresis loop reflecting a spot of mesopores at middle pressure area. The pore size distribution of OPS with a little pore volume showed that the most pores were in the range of 1.4 nm to 1.8 nm, which was estimated employing nonlocal density functional theory (NLDFT) (Fig. 3b). The pore structure of POPS-1 showed hierarchical pores with ultra micropore (less than 0.7 nm) and continuous mesopores. The POPS-2 also showed hierarchical pores distribution, but the mesopores were centred at 2.9 nm. Based on the above analysis, the Friedel-Crafts reaction using FDA as external crosslinker and Scholl coupling can effectively link the building blocks of OPS to obtain porous materials, respectively. From the table 1, the total pore volumes of POPS-1 and POPS-2 are 0.59 cm^3/g and 0.28 cm^3/g, respectively, but the microporosity of POPS-2 (39%) is higher than that of POPS-1 (22%). It may be due to the fact that the substantial cleavage of D4R cage of POPS-1 improves cage distortion in networks, which helps in increasing surface area and pore volume.[19]

Based on the increasing environmental concerns and energy demand, the H_2 storage and CO_2 capture have become one of the attractive topics in porous materials research. We, therefore, set out to investigate the potential of POPS-1 and POPS-2 in CO_2 capture at different temperatures (Fig. 4a and Fig. S5, ESI†). The CO_2 isotherms of POPS-1 and POPS-2 are shown in Figure 4a. Because of the similar porous structures of these two networks, the CO_2 isotherms of POPS-1 and POPS-2 are fairly consistent. At 273 K and 1 bar, the CO_2 uptake of POPS-1 and POPS-2 was found to be 9.73 wt% (2.21 mmol g^{-1}) and 8.12 wt% (1.84 mmol g^{-1}), respectively, which is comparable to that of COFs (1.21-3.84 mmol g^{-1}),[45] the PAFs (0.9-3.48 mmol g^{-1}),[46-48] and some hyper-crosslinked polymers (1.11-3.96 mmol g^{-1}).[14,49-54] The CO_2 uptake of POPS-1 and POPS-2 at 298 K are also more than that of POSS-based HPPs (0.62-1.04 mmol g^{-1}).[20,34] Furthermore, the CO_2 uptake of POPS-1 outperforms the commercially available BPL carbon (2.09 mmol g^{-1}). This excellent CO_2 uptake property may be attributed to the presence of silanol groups produced after the destruction of the D4R unit and the presence of abundant micropores. [55-57] Moreover, POPS-1 exhibits not only the

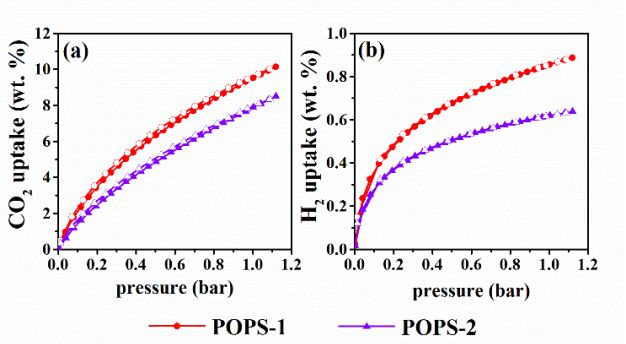

Figure 4. Volumetric CO_2 adsorption isotherms and desorption isotherms up to 1.13 bar at 273.15 K (a) and volumetric H_2 adsorption isotherms and desorption isotherms up to 1.13 bar at 77.3 K (b) of samples.

Table 1 porosity properties and gas uptake capacities of samples

No.	S_{BET}[a] (m^2/g)	S_L[b] (m^2/g)	PV[c] (cm^3/g)	MPV[d] (cm^3/g)	CO_2 uptake[e] (wt %)	H_2 uptake[f] (wt %)
OPS	9	13	0.06	0.0004	---	---
POPS-1	795	1078	0.59	0.13	9.73	0.89
POPS-2	472	627	0.28	0.11	8.12	0.64

[a] Surface area calculated from nitrogen adsorption isotherms at 77.3 K using BET equation. [b] Surface area calculated from nitrogen adsorption at 77 K using Langmuir equation. [c] Pore volume calculated from nitrogen isotherm at P/P_0=0.995, 77.3 K. [d] Micropore volume calculated from the nitrogen isotherm at P/P_0=0.050. [e] CO_2 uptake determined volumetrically using a micromeritics ASAP 2020 M analysis at 1.00 bar and 273.15 K. [f] H_2 uptake determined volumetrically using a micromeritics ASAP 2020 M analysis at 1.13 bar and 77.3 K.

highest gas uptake of these two porous networks, but also the highest isosteric heat (Q_{st}). According to the CO_2 sorption isotherms at 273 K and 298 K, the isosteric heat of POPS-1 and POPS-2 were found to be 24.4-27.9 kJ mol^{-1} and 22.4-23.4 kJ mol^{-1}, respectively. (Fig. S6, ESI†). Abundant micropores and silanol groups of porous material are helpful to increase the heat of adsorption. Compared to the isosteric heat of some PAFs and HCPs, the POPS-1 and POPS-2 showed the moderate values.[47] Based on moderate Q_{st} and the reversible sorption behaviour, the interactions of pore walls and CO_2 is weak, which allows the regeneration of polymer materials without heating.

Hydrogen, as a renewability energy, is a highly attractive candidate to reduce the pollution caused by fossil fuels. Based on the hydrogen sorption isotherms, we found that all isotherms were fully reversible and unsaturated at low pressures, and the hydrogen uptake capacities reached up to 0.89 wt % and 0.64 wt % for POPS-1 and POPS-2, respectively (Fig. 4b). These values are comparable to those of the some POSS-based porous materials, [31, 34] and other microporous polymers indicating their promising applications in gas uptake.[14, 58-61]

Conclusions

In summary, the POPS-1 and POPS-2 with high surface area were successfully prepared by simple Friedel-Crafts and Scholl coupling reactions respectively by using low-cost OPS as building blocks. It is worth noting that the abundant D4R cage structure of POSS was completely retained under relatively strong acidic conditions as confirmed by the FTIR and ^{29}Si MAS NMR analysis. Because of the low degree of hyper-crosslinking of POPS-2, the cage structure of POSS is basically integrated in the network. The gas sorption experiments show that the POPS-1 and POPS-2 are the promising materials for CO_2 uptake and hydrogen storage. The POPS-1 with BET surface area of 795 m^2 g^{-1}, can reversibly adsorb 9.73 wt% CO_2 (1 bar and 273 K) and 0.89 wt% H_2 (1.13 bar and 77 K). Given the relative low cost, the high surface area and the high thermal stability, these POSS-based networks are promising candidates for H_2 storage and CO_2 capture.

Acknowledgements

This work was financially supported by the program for National Natural Science Foundation of China (No. 21474033, 51273074, 51173058). We also thank the Analysis and Testing Center, Huazhong University of Science and Technology, for characterization assistance.

Notes and references

[a] Key Laboratory for Large-Format Battery Materials and System, Ministry of Education, School of Chemistry and Chemical Engineering, Huazhong University of Science and Technology, Luoyu Road No. 1037, Wuhan, 430074, China..

E-mail: bien.tan@mail.hust.edu.cn; fax: +862787543632; Tel: +862787558172.

† Electronic Supplementary Information (ESI) available: [details of any supplementary information available should be included here]. See DOI: 10.1039/b000000x/

[b] Key Laboratory for Large-Format Battery Materials and System, Ministry of Education, School of Chemistry and Chemical Engineering, Huazhong University of Science and Technology, Luoyu Road No. 1037, Wuhan, 430074, China.

[c] Department of Chemistry, SBA School of Science & Engineering (SSE), Lahore University of Management Sciences (LUMS), DHA, Lahore Cantt – 54792, Lahore, Pakistan

1. Q. Chen, M. Luo, P. Hammershoj, D. Zhou, Y. Han, B. W. Laursen, C. G. Yan and B. H. Han, *J. Am. Chem. Soc.*, 2012, **134**, 6084-6087.
2. Y. L. Luo, B. Y. Li, W. Wang, K. B. Wu and B. Tan, *Adv. Mater.*, 2012, **24**, 5703-5707.
3. B. Y. Li, Z. H. Guan, W. Wang, X. J. Yang, J. L. Hu, B. E. Tan and T. Li, *Adv. Mater.*, 2012, **24**, 3390-3395.
4. M. Seino, W. Wang, J. E. Lofgreen, D. P. Puzzo, T. Manabe and G. A. Ozin, *J. Am. Chem. Soc.,* 2011, **133**, 18082-18085.
5. C. Gu, N. Huang, J. Gao, F. Xu, Y. Xu and D. Jiang, *Angew. Chem. Int. Ed.*, 2014, **53**, 4850-4855.
6. F. Beguin, V. Presser, A. Balducci and E. Frackowiak, *Adv. Mater.*, 2014, **26**, 2219-2251.
7. W. Chaikittisilp, A. Sugawara, A. Shimojima and T. Okubo, *Chem. Eur. J.*, 2010, **16**, 6006-6014.
8. D. Wu, F. Xu, B. Sun, R. Fu, H. He and K. Matyjaszewski, *Chem. Rev.*, 2012, 112, 3959-4015.
9. M. Carta, P. Bernardo, G. Clarizia, J. C. Jansen and N. B. McKeown, *Macromolecules*, 2014, 47, 8320-8327..
10. P. Pachfule, S. Kandambeth, D. D. Diaz and R. Banerjee, *Chem. Commun.*, 2014, **50**, 3169-3172.
11. P. Katekomol, J. Roeser, M. Bojdys, J. Weber and A. Thomas, *Chem. Mater.*, 2013, **25**, 1542-1548.
12. K. Wu, J. Guo and C. Wang, *Chem. Commun.,* 2014, **50**, 695-697.
13. J. X. Jiang, Y. Y. Li, X. F. Wu, J. L. Xiao, D. J. Adams and A. I. Cooper, *Macromolecules*, 2013, **46**, 8779-8783.
14. B. Li, R. Gong, W. Wang, X. Huang, W. Zhang, H. Li, C. Hu and B. Tan, *Macromolecules*, 2011, **44**, 2410-2414.
15. Y. L. Luo, S. C. Zhang, Y. X. Ma, W. Wang and B. Tan, *Poly. Chem.*, 2013, **4**, 1126-1131.
16. T. Ben, H. Ren, S. Q. Ma, D. P. Cao, J. H. Lan, X. F. Jing, W. C. Wang, J. Xu, F. Deng, J. M. Simmons, S. L. Qiu and G. S. Zhu, *Angew. Chem. Int. Edit.*, 2009, **48**, 9457-9460.
17. M. P. Suh, H. J. Park, T. K. Prasad and D. W. Lim, *Chem. Rev.*, 2012, **112**, 782-835.
18. J. A. Greathouse and M. D. Allendorf, *J. Am. Chem. Soc.*, 2006, **128**, 10678-10679.
19. W. Chaikittisilp, M. Kubo, T. Moteki, A. Sugawara-Narutaki, A. Shimojima and T. Okubo, *J. Am. Chem. Soc.*, 2011, **133**, 13832-13835.
20. D. X. Wang, W. Y. Yang, L. G. Li, X. Zhao, S. Y. Feng and H. Z. Liu, *J. Mater. Chem. A*, 2013, **1**, 13549-13558.
21. D. B. Cordes, P. D. Lickiss and F. Rataboul, *Chem. Rev.*, 2010, **110**, 2081-2173.
22. Y. Wada, K. Iyoki, A. Sugawara-Narutaki, T. Okubo and A. Shimojima, *Chem. Eur. J.*, 2013, **19**, 1700-1705.
23. F. Alves and I. Nischang, *Chem. Eur. J.*, 2013, **19**, 17310-17313.
24. X. F. Jing, F. X. Sun, H. Ren, Y. Y. Tian, M. Y. Guo, L. N. Li and G. S. Zhu, *Microporous Mesoporous Mater.,* 2013, **165**, 92-98.
25. Y. Kim, K. Koh, M. F. Roll, R. M. Laine and A. J. Matzger, *Macromolecules*, 2010, **43**, 6995-7000.
26. J. J. Morrison, C. J. Love, B. W. Manson, I. J. Shannon and R. E. Morris, *J. Mater. Chem.*, 2002, **12**, 3208-3212.

27. Y. Peng, T. Ben, J. Xu, M. Xue, X. Jing, F. Deng, S. Qiu and G. Zhu, *Dalton trans.*, 2011, **40,** 2720-2724.
28. Y. Qin, H. Ren, F. Zhu, L. Zhang, C. Shang, Z. Wei and M. Luo, *Eur. Poly. J.*, 2011, **47**, 853-860.
29. D. Wang, L. Xue, L. Li, B. Deng, S. Feng, H. Liu and X. Zhao, *Macomol. Rapid commun.,* 2013, **34**, 861-866.
30. C. Zhang, F. Babonneau, C. Bonhomme, R. M. Laine, C. L. Soles, H. A. Hristov and A. F. Yee, *J. Am. Chem. Soc.*, 1998, **120**, 8380-8391.
31. W. Chaikittisilp, A. Sugawara, A. Shimojima and T. Okubo, *Chem. Mater.*, 2010, **22**, 4841-4843.
32. Y. Wu, D. Wang, L. Li, W. Yang, S. Feng and H. Liu, *J. Mater. Chem. A*, 2014, **2**, 2160-2167.
33. Y. C. Qin, F. H. Zhu, M. M. Luo and L. Zhang, *J. Appl. Poly. Sci.*, 2011, **121**, 97-101.
34. F. Alves, P. Scholder and I. Nischang, *ACS Appl. Mater. Interfaces,* 2013, **5**, 2517-2526.
35. B. Li, Z. Guan, X. Yang, W. D. Wang, W. Wang, I. Hussain, K. Song, B. Tan and T. Li, *J. Mater. Chem. A*, 2014, **2**, 11930-11939.
36. X. Yang, M. Yu, Y. Zhao, C. Zhang, X. Wang and J.-X. Jiang, *J. Mater. Chem. A*, 2014, **2**, 15139-15145.
37. X. Zhu, S. M. Mahurin, S.-H. An, C.-L. Do-Thanh, C. Tian, Y. Li, L. W. Gill, E. W. Hagaman, Z. Bian, J.-H. Zhou, J. Hu, H. Liu and S. Dai, *Chem. Commun.,* 2014, **50**, 7933-7936.
38. S. Yao, X. Yang, M. Yu, Y. Zhang and J.-X. Jiang, *J. Mater. Chem. A*, 2014, **2**, 8054-8059.
39. D. B. Cordes, P. D. Lickiss and F. Rataboul, Chem. Rev., 2010, 110, 2081-2173.
40. W. J. Malfait, R. Verel and M. M. Koebel, J. Phys. Chem. C, 2014, 118, 25545-25554.
41. D. Wang, W. Yang, S. Feng and H. Liu, Poly. Chem., 2014, 5, 3634-3642.
42. U. Diaz, T. Garcia, A. Velty and A. Corma, *Chem. Eur. J.*, 2012, **18**, 8659-8672.
43. K. S. W. Sing., D. H. Everett, R. A. W. Haul, L. Moscou, P. A. Pierotti, J. Rouquerol and T. Siemieniewska, *Pure Appl. Chem.,* 1985, **57**, 603-619.
44. J. Rouquerol., D. Avnir., C. W. Fairbridge., D. H. Everett., J. M. Haynes., N. Pernicone., J. D. F. Ramsay., K. S. W. Sing. and K. K. Unger., *Pure Appl. Chem.,* 1994, **66**, 1739-1758.
45. H. Furukawa and O. M. Yaghi, *J. Am. Chem. Soc.*, 2009, **131**, 8875-8883.
46. Z. J. Yan, H. Ren, H. P. Ma, R. R. Yuan, Y. Yuan, X. Q. Zou, F. X. Sun and G. S. Zhu, *Microporous Mesoporous Mater.*, 2013, **173**, 92-98.
47. T. Ben, C. Y. Pei, D. L. Zhang, J. Xu, F. Deng, X. F. Jing and S. L. Qiu, *Energy Environ. Sci.*, 2011, **4**, 3991-3999.
48. H. P. Ma, H. Ren, X. Q. Zou, S. Meng, F. X. Sun and G. S. Zhu, *Poly. Chem.*, 2014, **5**, 144-152.
49. R. Dawson, L. A. Stevens, T. C. Drage, C. E. Snape, M. W. Smith, D. J. Adams and A. I. Cooper, *J. Am. Chem. Soc.*, 2012, **134**, 10741-10744.
50. R. Dawson, T. Ratvijitvech, M. Corker, A. Laybourn, Y. Z. Khimyak, A. I. Cooper and D. J. Adams, *Poly. Chem.*, 2012, **3**, 2034.
51. R. Dawson, E. Stöckel, J. R. Holst, D. J. Adams and A. I. Cooper, *Energy Environ. Sci.*, 2011, **4**, 4239.
52. R. Dawson, A. I. Cooper and D. J. Adams, *Prog. Poly. Sci.*, 2012, **37**, 530-563.
53. S. J. Xu, Y. L. Luo and B. E. Tan, *Macromol. Rapid communi.*, 2013, **34**, 471-484.
54. C. F. Martin, E. Stockel, R. Clowes, D. J. Adams, A. I. Cooper, J. J. Pis, F. Rubiera and C. Pevida, *J. Mater. Chem.,* 2011, **21**, 5475-5483.
55. R. Dawson, A. I. Cooper and D. J. Adams, Polym. Int, 2013, 62, 345-352.
56. R. Dawson, D. J. Adams and A. I. Cooper, Chem. Sci., 2011, 2, 1173-1177.
57. W. Lu, D. Yuan, J. Sculley, D. Zhao, R. Krishna and H. C. Zhou, J. Am. Chem. Soc., 2011, 133, 18126-18129.
58. R. Dawson, A. Laybourn, R. Clowes, Y. Z. Khimyak, D. J. Adams and A. I. Cooper, *Macromolecules*, 2009, **42**, 8809-8816.
59. C. Zhang, Z. Wang, J. J. Wang, L. X. Tan, J. M. Liu, B. Tan, X. L. Yang and H. B. Xu, *Polymer*, 2013, **54**, 6942-6946.
60. Y. Luo, B. Li, L. Liang and B. Tan, *Chem. Commun.*, 2011, **47**, 7704-7706.
61. Y. C. Zhao, L. M. Zhang, T. Wang and B. H. Han, *Poly. Chem.*, 2014, **5**, 614-621.

Table of contents entry

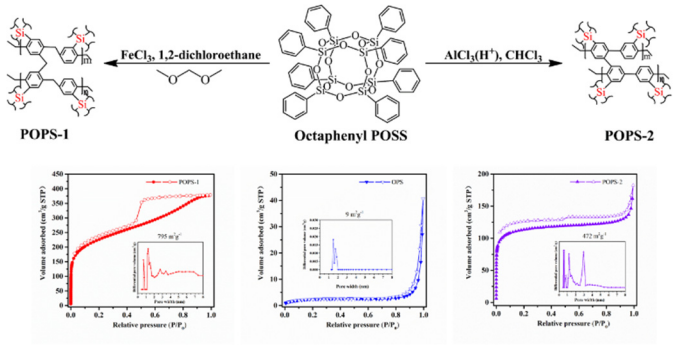

POSS-based organic-inorganic hybrid porous materials by low cost strategy